Controlled Manipulation of Bacteriophages Using Single-Virus Force Spectroscopy

David Alsteens,[†,§] Emanuele Pesavento,[‡,§] Gilles Cheuvart,[†] Vincent Dupres,[†] Heykel Trabelsi,[‡] Patrice Soumillion,[‡,*] and Yves F. Dufrêne[†,*]

[†]Unité de Chimie des Interfaces, Université Catholique de Louvain, Croix du Sud 2/18, B-1348 Louvain-la-Neuve, Belgium, and [‡]Laboratoire d'Ingénierie des Protéines et des Peptides, Institut des Sciences de la Vie, Université Catholique de Louvain, Croix du sud 4/5, B-1348 Louvain-la-Neuve, Belgium. [§]D.A. and E.P. contributed equally to this work.

ABSTRACT A method is described for the site-directed manipulation of single filamentous bacteriophages, by using phage display technology and atomic force microscopy. f1 filamentous bacteriophages were genetically engineered to display His-tags on their pIX tail. Following adsorption on nitrilotriacetate-terminated surfaces, force spectroscopy with tips bearing monoclonal anti-pIII antibodies was used to pull on individual phages *via* their pIII head. Analysis of the force-extension profiles revealed that upon pulling, the phages are progressively straightened into an extended orientation until rupture of the anti-pIII/pIII complex. The single-virus manipulation technique presented here provides new opportunities for understanding the forces driving cell—virus and material—virus interactions, and for characterizing the binding properties of polypeptide sequences or proteins selected by the phage display technology.

KEYWORDS: phage display · bacteriophages · single virus manipulation · atomic force microscopy · force spectroscopy

Filamentous bacteriophages, which include f1, fd, and M13 species, are able to infect a variety of Gram-negative bacteria like *Escherichia coli*.[1−3] These phages share a common morphology and a circular, single-stranded DNA genome. In contrast to lytic bacteriophages, filamentous phages are assembled in the cytoplasmic membrane and secreted from infected bacteria without cell lysis. Infection begins by the attachment of proteins pIII to the F pilus of a male *E. coli*. The circular single-stranded DNA enters the bacteria where it is converted by the host DNA replication machinery into a double-stranded plasmid replicative form. By rolling circle replication, the replicative form makes single-stranded DNA, and the templates for expression of the coat proteins are formed. These proteins are inserted into the cytoplasmic membrane, waiting for phage extrusion. Finally, morphogenesis and extrusion of phage descendants occur simultaneously by packaging of the single-stranded DNA into coat proteins while the filamentous particle crosses the bacterial wall.[1,2]

Phage display technology, first introduced by G.P. Smith[3] in 1985, permits the presentation of large peptide and protein libraries on the surface of filamentous phages, which affords the *in vitro* selection of peptides and proteins (including antibodies) with high affinity and specificity to almost any target by affinity capture.[4,5] Phage display involves the fusion of foreign DNA sequences to the phage genome such that the resulting foreign proteins are expressed in fusion with one of the coat proteins. Although all five coat proteins have been used to display proteins or peptides, gene VIII protein (pVIII) and gene III protein (pIII) are by far the most commonly used. Notably, filamentous bacteriophages engineered by phage display also offer exciting opportunities in nanotechnology, for example, for the directed synthesis of magnetic and semiconducting nanowires[6,7] and for the assembly of functional hybrid nanostructures.[8]

While classical biophysical and molecular biology techniques probe the averaged properties of viruses, single molecule assays provide a means to observe, analyze, and manipulate individual virus particles, thereby revealing events and properties that would otherwise be hidden.[9−12] In this context, recent progress in atomic force microscopy (AFM) methods[13,14] has enabled researchers to image a variety of viruses in buffer solution,[15−18] and to measure the forces required to detach them from cell membranes.[12] Yet, the combined use of genetic engineering and AFM for the site-directed manipulation of filamentous phages has never been reported.

*Address correspondence to yves.dufrene@uclouvain.be, patrice.soumillion@uclouvain.be.

Received for review July 10, 2009 and accepted September 10, 2009.

Published online September 21, 2009.
10.1021/nn900778t CCC: $40.75

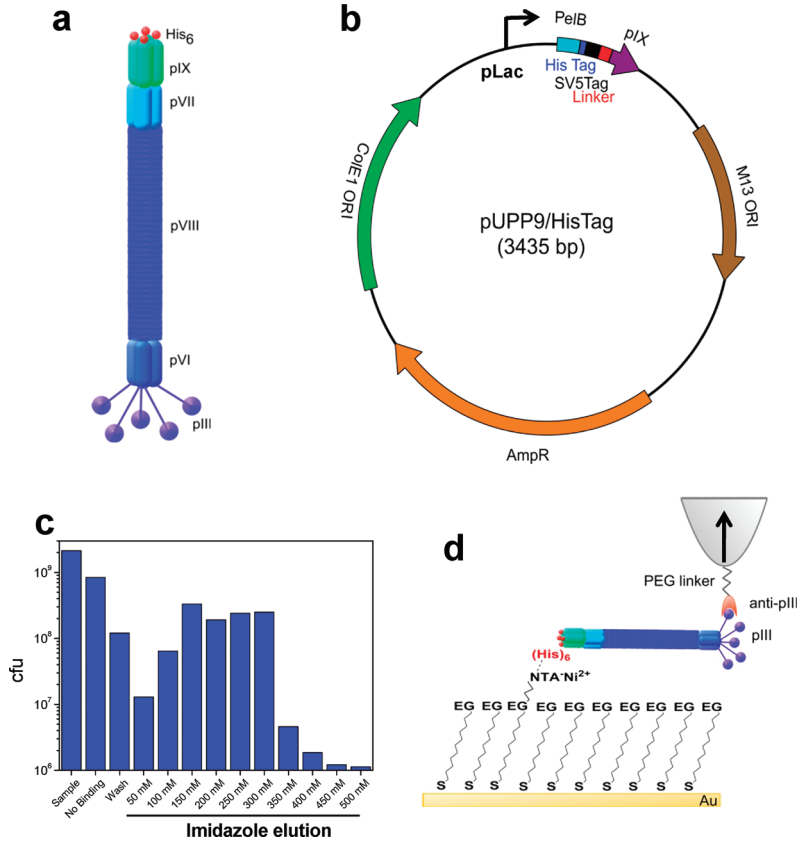

Figure 1. Principle of site-directed single-virus manipulation. (a) Ff filamentous bacteriophages are genetically engineered to display His-tags on their pIX tail. (b) To this end, *E. coli* bacteria are transformed by a phagemid (pUPP9/HisTag) which code for a His_6-pIX protein and infected by a helper phage. (c) The solution of His-tagged phage particles is purified by immobilized ion metal affinity chromatography. In the various input and output fractions, phage particles are detected by their infectivity and titrated as colony forming units (cfu). Approximately 50% of the particles are retained on the column and can be eluted by competition with imidazole. Purified phages are collected by pooling the eluted fractions ranging from 150 to 300 mM imidazole. (d) Following extensive purification, the heterobifunctional filaments are anchored *via* their His-pIX tail on gold surfaces modified with NTA/EG groups and picked through their pIII head using an AFM tip modified with anti-pIII antibodies.

RESULTS AND DISCUSSION

To address this challenge, we genetically engineered filamentous bacteriophages to display His_6 tags at their pIX, N terminal tail (Figure 1a). We achieved this by using *E. coli* bacteria infected by a R408 helper phage, a f1-type phage,[19] and transformed with a phagemid which code for a His_6-pIX protein (Figure 1b). The obtained tagged filamentous particles are a mixture of R408 helper phage and encapsidated ssDNA of pUPP9/HisTag phagemids. They were precipitated together by polyethylene glycol (PEG) and further purified on a Ni^{2+}-NTA column with a ~50% yield (Figure 1c). The successful purification by immobilized metal affinity chromatography confirms the efficient His_6 tag display on the phage particles and also affords a high purity that is required for subsequent AFM analysis. Phages were then attached *via* their His_6 tags on gold surfaces modified with nitrilotriacetate (NTA) groups and picked through their pIII head using an AFM tip modified with anti-pIII antibodies (Figure 1d).

The quality of the phage production and purification procedures was first assessed by AFM imaging (Figure 2). Figure 2 panels a and b show AFM images of mica surfaces on which engineered phages were adsorbed. The surfaces were devoid of large aggregates or debris and clearly showed individual, slightly curved filaments of 7 ± 2 nm diameter (Figure 2c) and 400−1000 nm length. Overall, these values fit with the theoretical dimensions of the engineered phages. Since the phage length is proportional to the size of the encapsidated DNA,[4] we expect their theoretical contour length, L_c, to be either 500 or 930 nm, depending whether they result from the insertion of the ssDNA from the phagemid or from the helper phage. Last, as we shall see below, it is convenient for further interpretation of the force measurements to take into account the curvature of the filaments and to estimate, from the images, a characteristic distance as the crow flies corresponding to the head-to-tail length of the immobilized phages (L_{ht}). As can been seen in Figure 2d, the distribution of L_{ht} values showed two maxima centered at 480 and 825 nm, corresponding most probably to the phagemid and phage helper particles, respectively. We note that samples that were only purified by PEG precipitation (thus without passage on Ni^{2+}-NTA column) were of very poor quality; that is, numerous aggregates were observed, presumably resulting from the coprecipitation of bacterial debris and phage particles. These data demonstrate that thorough purification (PEG precipitation + Ni^{2+}-NTA column) of the phages is essential for observing individual viruses and for guaranteeing further reliable single-virus measurements.

Force spectroscopy was then used to pull on the pIII head of individual phages anchored on NTA/EG surfaces (Figure 1d). To this end, AFM tips were functionalized with monoclonal anti-pIII antibodies, using a flexible polyethylene glycol spacer which permits the antibodies to be firmly attached and to be freely oriented. Shown in Figure 3 are the force data obtained between anti-pIII tips and phage surfaces. In 35% of the cases (n = 360), the curves showed either single or multiple binding peaks, together with rupture lengths ranging from 50 nm to several hundreds nm. The distribution of the last adhesion forces (F_{adh}), showed a well-defined maximum at 44 ± 14 pN (n = 360) that we attribute to specific antibody−antigen interactions for the following rea-

sons: (i) this force value is much smaller than the 150 pN force associated with single His-Ni^{2+}-NTA bonds;[20] (ii) a marked reduction of adhesion frequency was observed when force curves were recorded in 200 μg/mL solutions of anti-pIII (Figure 3b, inset). In view of the tip surface chemistry that we used (PEG linker) and of the fact that our measured forces are in the range of values reported for single antigen−antibody interactions using similar recording conditions,[21−25] we conclude that the 44 pN force is likely to reflect the rupture of single pIII/anti-pIII complexes. Adhesion forces in the 50−100 pN range were frequently observed and attributed to the simultaneous detection of two pIII proteins, in agreement with the notion that each phage displays multiple copies of pIII proteins.

Consistent with the above observations, we found that the mean adhesion force (F) increased linearly with the logarithm of the loading rate (r), as expected for specific interactions (Figure 3c).[23−25] From this relationship, the length scale of the energy barrier was assessed from the slope of the F *versus* ln(r) plot, $x_\beta = 0.77$ nm, while extrapolation to zero forces yielded the kinetic off-rate constant of dissociation at zero force, $k_{off} = r_{F=0}\, x_\beta / k_B T = 0.74\ s^{-1}$. Both x_β and k_{off} values are in the range of values reported in previous antigen−antibody studies ($x_\beta = 0.4-1.0$ nm and $k_{off} = 10^{-3}-10^{2}\ s^{-1}$).[22,26,27]

We also note that the 35% binding probability is larger than what we expect considering the surface coverage of the bacteriophages observed in air (Figure 2a). There are several possible reasons for this apparent discrepancy. First, during force measurements some viruses may protrude into the solution with a certain degree of mobility since they are only attached *via* their pIX tail. We therefore speculate that an anti-pIII tip may detect the same pIII head multiple times. Second, due to dewetting forces associated with drying, the surface density of the bacteriophages may be smaller in air than in liquid. Accordingly, the above data show that AFM with anti-pIII tips can detect and manipulate single bacteriophages *via* their pIII head up to a maximum force of 150 pN (strength of the His-Ni^{2+}-NTA bond), therefore validating the proof-of-concept of "site-directed single-virus force spectroscopy".

Another pertinent issue is to understand the molecular origin of the force peak profiles (shape, rupture length). Notably, we found that none of the force peaks could be described by the wormlike-chain (WLC) model, which is in contrast with the behavior of modular proteins. Force-extension curves of such proteins generally show nonlinear force peaks that can be fitted by the WLC model, each peak reflecting the force-induced unfolding of secondary structures (α-helices, β-sheets).[28−32] Thus, rather than reflecting secondary structure deformations, we suggest that the intermediate force jumps correspond to the progressive desorption of the filaments from the surface and/or from neighboring phages (see the image in Figure 2a showing that some phages associate with each other), while the last jump represents the rupture of the pIII−antipIII complex.

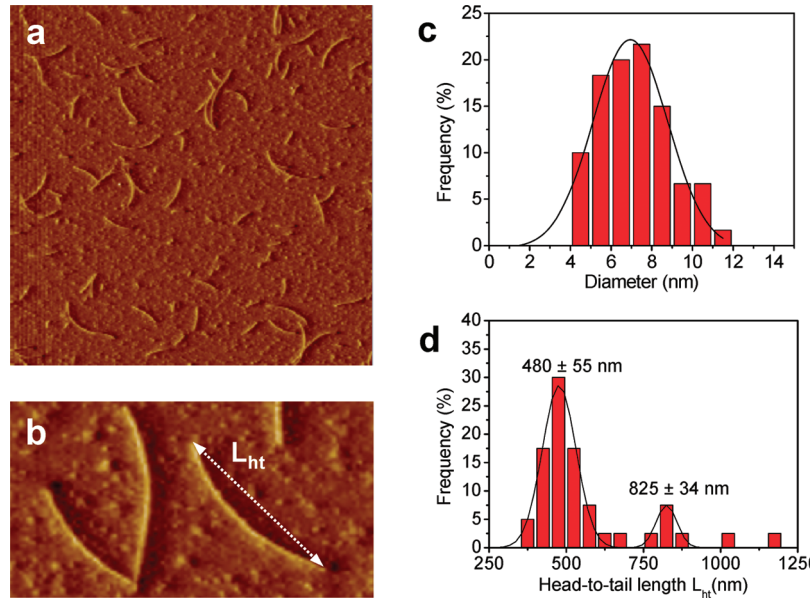

Figure 2. AFM imaging of single viruses. (a,b) Deflection images in air of genetically engineered phages adsorbed on mica (image size: 10 μm × 10 μm (a) and 3 μm × 1.6 μm (b)). Statistical analysis of (c) the diameter and (d) head-to-tail length (L_{ht}, see arrow in Figure 2b) of single filaments (measured on 60 filaments from five images).

How about the origin of the observed rupture lengths? Figure 3d shows that the average rupture length was $L_r = 128 \pm 52$ nm, which is much smaller than the phage length, $L_c = 500$ nm. However, the L_r values can be easily interpreted considering the following model (Figure 3e): (i) initially, the engineered phage is a rigid rod[10] that is slightly curved; (ii) upon pulling on its pIII head, it progressively looses its curvature and become more extended since the pIX tail remains attached on the surface. As there is no lateral motion of the tip or the surface, rupture should take place when the phage is in straight oblique position between the His-Ni-NTA and pIII/anti-pIII anchor points. Considering our mean experimental values $L_{ht} = 480$ nm and the theoretical contour length $L_c = 500$ nm, we find that the expected rupture length should be 140 nm, which matches remarkably well the experimental data, $L_r \approx 130$ nm. The above interpretation is further supported by a controlled experiment in which the phages were attached randomly and *via* multiple points on surfaces using PEG linkers. In these conditions, the average rupture length dropped to $L_r = 18 \pm 10$ nm (Figure 3d; inset), a value which corresponds to the extension of the

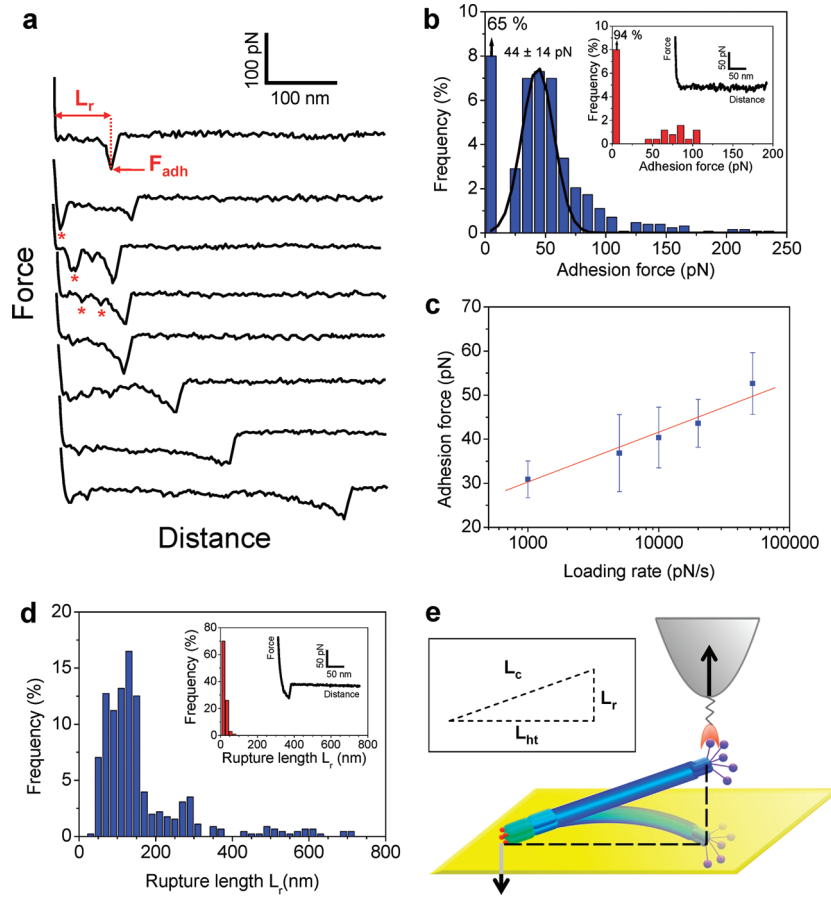

Figure 3. Site-directed force spectroscopy of single viruses. (a) Representative force curves recorded in buffer solution between genetically engineered phages anchored on a NTA/EG surface and AFM tips functionalized with anti-pIII. The last force peak represents the adhesion force of the anti-pIII/pIII pair (see "F_{adh}" label), while the occasional intermediate force jumps are attributed to phage-surface or phage−phage desorption events (see asterisk (*) labels). Although most rupture lengths (L_r) were around 100 nm, some were up to several hundreds nm (lower traces). Data obtained using an approach speed of 1000 nm s^{-1} and an interaction time of 500 ms. (b) Histogram showing the distribution of the last adhesion forces (F_{adh}) generated from 1024 curves. The curves were obtained by recording, on 10 μm × 10 μm areas, four force−volume data sets consisting each of 16 × 16 force curves. Three different tips and three different surfaces prepared independently were used. Shown in the inset is a blocking experiment performed in a 200 μg/mL solution of anti-pIII. The histogram was obtained by recording two 16 × 16 force−volume data sets, using two tips and two surfaces prepared independently. (c) Dependence of the adhesion force on the loading rate applied during retraction. The interaction time (500 ms) and the approach speed (1000 nm s^{-1}) were kept constant. (d) Histogram showing the distribution of rupture length (L_r) from 360 different curves. Shown in the inset is the distribution of L_r values observed when the phages were attached *via* multiple points using PEG linkers. (e) Schematics of the single-virus pulling experiment: initially, the phages are slightly curved and lying flat on the surface; upon pIII detection and pulling, they are straightened into an extended orientation.

PEG linkers on the tip and on the surface, and to the stretching of the pIII/anti-pIII complex. Together, these findings show that single filaments were manipulated and extended *via* their two terminal regions, without deformations of the constituting proteins (unfolding, depolymerization).

CONCLUSIONS

In conclusion, our experiments demonstrate that the combined used of phage display technology and AFM is a powerful platform for the controlled manipulation of individual filamentous bacteriophages. Pulling on the pIII head of bacteriophages anchored by their pIX tail using moderate forces, leads to their progressive desorption from the surface and to their straightening into an extended orientation. We anticipate that the novel method presented here, that is, site-directed single-virus force spectroscopy, will find broad applications in life science and nanotechnology. In biology, the site-directed manipulation of bacteriophages with AFM tips should allow the exploration of the forces that drive the various stages of the bacterial infection process (attachment of pIII proteins to F pili and assembly and secretion of the phages from the bacterial surface). In bio- and nanotechnology, the method should be very useful to characterize the biophysical properties of engineered phages particles and phage displayed peptides or proteins that bind to specific bioligands or to organics/inorganics used for the design of self-assembled hybrid materials.[8]

METHODS

Chemicals and Biologicals. Polyethylene glycol 6000 was purchased from AppliChem (Germany) and other chemicals from Sigma Aldrich (Germany). His Trap FF columns were from GE Healthcare Life Science. *E. coli* strain TG1 is from Invitrogen.

Construction of the Phage Expressing HisTag on pIX. The HisTag coding sequence was obtained by annealing the oligos His/F (5′-GCGC**GCATGC**CGCACACCATCACCATCACCATGCTAGCGGC-3′) and His/R (5′-GCCGCTAGCATGGTGATGGTGATGGTGTGCG-GCATGCGCGC-3′). A fragment encoding SV5Tag-linker-pIX-*Eco*RI was isolated by PCR from a plasmid expressing a GFP-pIX fusion protein (E. Pesavento, unpublished work) using the primers SV5/F (5′-CACCATGCTAGCGGCAAACCAATCCC-3′) and pUC/R (5′-CGACGTTGTAAAACGACGG-3′). The HisTag and SV5Tag-linker-pIX-*Eco*RI fragments were then assembled by overlap PCR using His/F and pUC/R as primers. In this way, an ORF composed of HisTag- SV5Tag-linker-pIX, flanked by *Sph*I and *Eco*RI restriction sites, was obtained. This ORF was cloned in a pDAN5-sfGFP vector (A. Bradbury, to be published) in place of the sfGFP-pIII ORF. The pDan5-sfGFP vector is based on a pUC19 plasmid with an M13_origin. The resulting phagemid, named pUPP9-HisTag (Figure 1b), was electroporated into *E. coli* TG1.

Phage Production and Purification. One liter of LB-Ampicillin (100 μg/mL) medium inoculated by TG1 harboring the phagemid pUPP9His/Tag and already infected by the helper phage R408 was grown overnight at 37 °C. After centrifugation, the phages were purified from the supernatant by two successive PEG precipitations. The final pellet was dissolved in 1 mL of Milli-Q water and reprecipitated again for 20 min at 4 °C with 200 μL of PEG/NaCl (20% W/V PEG 6000/2.5 M NaCl). The mixture was centrifuged at 10000 rpm for 20 min at 4 °C and the precipitated phage was finally dissolved in 2 mL of Milli-Q water. This phage sample was loaded onto the His Trap FF column (prepacked with Ni sepharose) beforehand, prepared as recommended by the manufacturer's protocols, and equilibrated at a flow rate of 1 mL/min with the equilibration buffer (50 mM Tris-HCl, 100 mM NaCl, and 20 mM Imidazole pH 7.4). After washing the column with five volumes of equilibration buffer the his tagged phages were eluted with a 50 mM stage imidazole gradient (starting from 50 up to 450 mM) in the same buffer.

Phage Titer Measurements. Serial 10× dilutions of the purified phagemid particles were prepared and 10 μL of each one were mixed with 990 μL of a TG1 culture in exponential phase. After incubation at 37 °C without agitation for 30 min and with agitation for another 30 min, 100 μL of each mixture were spread on LB Petri dishes containing Ampicillin (100 μg/mL) and incubated overnight at 37 °C. The colonies were counted and the phage titer was calculated as colony-forming-units (cfu).

AFM Measurements. AFM measurements were performed at 20 °C in buffered solutions (PBS, pH 7.4), using a Nanoscope IV Multimode AFM (Veeco Metrology Group, Santa Barbara, CA) and oxide sharpened microfabricated Si_3N_4 cantilevers (Microlevers, Veeco Metrology Group). Force measurements were recorded in the force−volume mode consisting of arrays of 16 × 16 force curves on 10 μm × 10 μm areas, using a maximum applied force of 350 pN and a loading rate of 10000 pN/s, calculated by multiplying the tip pulling velocity (nm/s) by the slope of the peaks (pN/nm). A ramp delay of 500 ms was applied between tip approach and tip retraction, while keeping constant the maximum applied force. The spring constants of the cantilevers were measured using the thermal noise method (Picoforce, Veeco Metrology Group), yielding values ranging from 0.01 to 0.015 N/m. Force-volume data were treated using the Nanoscope V 7.30 (Veeco Metrology Group) and Matlab (The Mathworks Inc.) softwares.

For force spectroscopy, AFM tips were functionalized with anti-pIII (Mo Bi Tec, Germany) using PEG-benzaldehyde linkers provided by H.J. Gruber (University of Linz), essentially as described elsewhere.[33] Cantilevers were washed with chloroform and ethanol, placed in an UV−ozone cleaner for 30 min, immersed overnight into an ethanolamine solution (3.3 g ethanolamine into 6 mL of DMSO), then washed three times with DMSO and two times with ethanol, and dried with N_2. The ethanolamine-coated cantilevers were immersed for 2 h in a solution prepared by mixing 1 mg of Acetal-PEG-NHS dissolved in 0.5 mL of chloroform with 10 μL of triethylamine, then washed with chloroform and dried with N_2. Cantilevers were further immersed for 5 min in a 0.1% iodine/acetone solution, washed three times in acetone, dried under N_2, and then covered with a 200 μL droplet of a PBS solution containing anti-pIII (0.2 mg/mL) to which 2 μL of a 1 M $NaCNBH_3$ solution were added. After 50 min, cantilevers were incubated with 5 μL of a 1 M ethanolamine solution in order to passivate unreacted aldehyde groups, and then washed with and stored in PBS 10 min later.

For surface immobilization of the phages, silicon wafers (Siltronix) were coated using electron beam thermal evaporation with a 5-nm thick chromium layer followed by a 30-nm thick gold layer. The gold-coated surfaces were cleaned for 15 min by UV and ozone treatment, rinsed with ethanol, dried with a gentle nitrogen flow, and immersed overnight in ethanol containing 0.05 mM of NTA-terminated (10%) and triethylene glycol(EG)-terminated (90%) alkanethiols. After rinsing with ethanol, the tips and supports were immersed in a 40 mM aqueous solution of $NiSO_4$ (pH 7.2) for 1 h, rinsed with water, incubated in 1 mL of purified phage solution for 2 h, and finally rinsed with PBS. After rinsing, the support was carefully attached to a steel sample puck (Veeco Metrology Group) using a small piece of double face adhesive tape, and the mounted sample was transferred into the AFM liquid cell while avoiding dewetting.

Acknowledgment. The pDAN5-sfGFP phagemid was a kind gift of Andrew Bradbury. We thank H. J. Gruber for providing us with the PEG linkers. This work was supported by the National Foundation for Scientific Research (FNRS), the Université catholique de Louvain (Fonds Spéciaux de Recherche), the Région wallonne (Pôle d'excellence NANOTIC), the Federal Office for Scientific, Technical and Cultural Affairs (Interuniversity Poles of Attraction Programme), and the Research Department of the Communauté française de Belgique (Concerted Research Action). Y.F.D. and D.A. are Senior Research Associate and Research Fellow of the FRS-FNRS.

REFERENCES AND NOTES

1. Marvin, D. A. Filamentous Phage Structure, Infection, and Assembly. *Curr. Opin. Struct. Biol.* **1998**, *8*, 150–158.
2. Russel, M.; Linderoth, N. A.; Sali, A. Filamentous Phage Assembly: Variation on a Protein Export Theme. *Gene* **1997**, *192*, 23–32.
3. Smith, G. P. Filamentous Fusion Phage: Novel Expression Vectors that Display Cloned Antignes on the Virion Surface. *Science* **1985**, *228*, 1315–1317.
4. Minard, P.; Urvoas, A.; Soumillion, P. , Protein Engineering by Phage Display. In *Protein Engineering Handbook*; Lutz, S., Bornscheuer, U., Eds.; Wiley-VCH Verlag Gmbh: Weinheim, Germany, 2008; pp 563−604.
5. Kehoe, J. W.; Kay, B. K. Filamentous Phage Display in the New Millennium. *Chem. Rev.* **2005**, *105*, 4056–4072.
6. Mao, C. B.; Flynn, C. E.; Hayhurst, A.; Sweeney, R.; Qi, J. F.; Georgiou, G.; Iverson, B.; Belcher, A. M. Viral Assembly of Oriented Quantum Dot Nanowires. *Proc. Natl. Acad. Sci. U.S.A.* **2003**, *100*, 6946–6951.
7. Mao, C. B.; Solis, D. J.; Reiss, B. D.; Kottmann, S. T.; Sweeney, R. Y.; Hayhurst, A.; Georgiou, G.; Iverson, B.; Belcher, A. M. Virus-Based Toolkit for the Directed Synthesis of Magnetic and Semiconducting Nanowires. *Science* **2004**, *303*, 213–217.
8. Sarikaya, M.; Tamerler, C.; Jen, A. K. Y.; Schulten, K.; Baneyx, F. Molecular Biomimetics: Nanotechnology through Biology. *Nat. Mater.* **2003**, *2*, 577–585.
9. Ashkin, A.; Dziedzic, J. M. Optical Trapping and Manipulating of Viruses and Bacteria. *Science* **1987**, *235*, 1517–1520.
10. Khalil, A. S.; Ferrer, J. M.; Brau, R. R.; Kottmann, S. T.; Noren, C. J.; Lang, M. J.; Belcher, A. M. Single M13 Bacteriophage Tethering and Stretching. *Proc. Natl. Acad. Sci. U.S.A.* **2007**, *104*, 4892–4897.
11. Ivanovska, I. L.; de Pablo, P. J.; Ibarra, B.; Sgalari, G.; MacKintosh, F. C.; Carrascosa, J. L.; Schmidt, C. F.; Wuite,

G. J. L. Bacteriophage Capsids: Tough Nanoshells with Complex Elastic Properties. *Proc. Natl. Acad. Sci. U.S.A.* **2004**, *101*, 7600–7605.
12. Rankl, C.; Kienberger, F.; Wildling, L.; Wruss, J.; Gruber, H. J.; Blaas, D.; Hinterdorfer, P. Multiple Receptors Involved in Human Rhinovirus Attachment to Live Cells. *Proc. Natl. Acad. Sci. U.S.A.* **2008**, *105*, 17778–17783.
13. Muller, D. J.; Dufrene, Y. F. Atomic Force Microscopy as a Multifunctional Molecular Toolbox in Nanobiotechnology. *Nat. Nanotechnol.* **2008**, *3*, 261–269.
14. Muller, D. J.; Helenius, J.; Alsteens, D.; Dufrene, Y. F. Force Probing Surfaces of Living Cells to Molecular Resolution. *Nat. Chem. Biol.* **2009**, *5*, 383–390.
15. Muller, D. J.; Engel, A.; Carrascosa, J. L.; Velez, M. The Bacteriophage Phi 29 Head−Tail Connector Imaged at High Resolution with the Atomic Force Microscope in Buffer Solution. *EMBO J.* **1997**, *16*, 2547–2553.
16. Kuznetsov, Y. G.; Malkin, A. J.; Lucas, R. W.; Plomp, M.; McPherson, A. Imaging of Viruses by Atomic Force Microscopy. *J. Gen. Virol.* **2001**, *82*, 2025–2034.
17. Malkin, A. J.; McPherson, A.; Gershon, P. D. Structure of Intracellular Mature Vaccinia Virus Visualized by *in Situ* Atomic Force Microscopy. *J. Virol.* **2003**, *77*, 6332–6340.
18. Kienberger, F.; Rankl, C.; Pastushenko, V.; Zhu, R.; Blaas, D.; Hinterdorfer, P. Visualization of Single Receptor Molecules Bound to Human *Rhinovirus* under Physiological Conditions. *Structure* **2005**, *13*, 1247–1253.
19. Russel, M.; Kidd, S.; Kelley, M. R. An Improved Filamentous Helper Phage for Generating Single-Stranded Plasmid DNA. *Gene* **1986**, *45*, 333–338.
20. Verbelen, C.; Gruber, H. J.; Dufrene, Y. F. The NTA-His(6) Bond Is Strong Enough for AFM Single-Molecular Recognition Studies. *J. Mol. Recognit.* **2007**, *20*, 490–494.
21. Berquand, A.; Xia, N.; Castner, D. G.; Clare, B. H.; Abbott, N. L.; Dupres, V.; Adriaensen, Y.; Dufrêne, Y. F. Antigen Binding Forces of Single Antilysozyme Fv Fragments Explored by Atomic Force Microscopy. *Langmuir* **2005**, *21*, 5517–5523.
22. Ros, R.; Schwesinger, F.; Anselmetti, D.; Kubon, M.; Schafer, R.; Pluckthun, A.; Tiefenauer, L. Antigen Binding Forces of Individually Addressed Single-Chain Fv Antibody Molecules. *Proc. Natl. Acad. Sci. U.S.A.* **1998**, *95*, 7402–7405.
23. Schwesinger, F.; Ros, R.; Strunz, T.; Anselmetti, D.; Guntherodt, H. J.; Honegger, A.; Jermutus, L.; Tiefenauer, L.; Pluckthun, A. Unbinding Forces of Single Antibody−Antigen Complexes Correlate with Their Thermal Dissociation Rates. *Proc. Natl. Acad. Sci. U.S.A.* **2000**, *97*, 9972–9977.
24. Verbelen, C.; Christiaens, N.; Alsteens, D.; Dupres, V.; Baulard, A. R.; Dufrene, Y. F. Molecular Mapping of Lipoarabinomannans on Mycobacteria. *Langmuir* **2009**, *25*, 4324–4327.
25. Morfill, J.; Neumann, J.; Blank, K.; Steinbach, U.; Puchner, E. M.; Gottschalk, K.-E.; Gaub, H. E. Force-Based Analysis of Multidimensional Energy Landscapes: Application of Dynamic Force Spectroscopy and Steered Molecular Dynamics Simulations to an Antibody Fragment-Peptide Complex. *J. Mol. Biol.* **2008**, *381*, 1253–1266.
26. Merkel, R.; Nassoy, P.; Leung, A.; Ritchie, K.; Evans, E. Energy Landscapes of Receptor-Ligand Bonds Explored with Dynamic Force Spectroscopy. *Nature* **1999**, *397*, 50–53.
27. Evans, E.; Ritchie, K. Dynamic Strength of Molecular Adhesion Bonds. *Biophys. J.* **1997**, *72*, 1541–1555.
28. Sotomayor, M.; Schulten, K. Single-Molecule Experiments *in Vitro* and *in Silico*. *Science* **2007**, *316*, 1144–1148.
29. Rief, M.; Gautel, M.; Oesterhelt, F.; Fernandez, J. M.; Gaub, H. E. Reversible Unfolding of Individual Titin Immunoglobulin Domains by AFM. *Science* **1997**, *276*, 1109–1112.
30. Oberhauser, A. F.; Marszalek, P. E.; Erickson, H. P.; Fernandez, J. M. The Molecular Elasticity of the Extracellular Matrix Protein Tenascin. *Nature* **1998**, *393*, 181–185.
31. Oesterhelt, F.; Oesterhelt, D.; Pfeiffer, M.; Engel, A.; Gaub, H. E.; Muller, D. J. Unfolding Pathways of Individual Bacteriorhodopsins. *Science* **2000**, *288*, 143–146.
32. Alsteens, D.; Dupres, V.; Klotz, S. A.; Gaur, N. K.; Lipke, P. N.; Dufrêne, Y. F. Unfolding Individual Als5p Adhesion Proteins on Live Cells. *ACS Nano* **2009**, *3*, 1677–1682.
33. Ebner, A.; Wildling, L.; Kamruzzahan, A. S. M.; Rankl, C.; Wruss, J.; Hahn, C. D.; Holzl, M.; Zhu, R.; Kienberger, F.; Blaas, D.; *et al*. A New, Simple Method for Linking of Antibodies to Atomic Force Microscopy Tips. *Bioconjugate Chem.* **2007**, *18*, 1176–1184.